Managing emergent recovery dynamics in at-risk metapopulations

Supplemental materials: Model details & results

Kyle L. Wilson[1,2]*, Alexandra C. Sawyer[1], Anna Potapova[1], Colin J. Bailey[1], Daniella LoScerbo[3,4],
Elissa K. Sweeney-Bergen[1,5], Emma E. Hodgson[1,4], Kara J. Pitman[1], Karl M. Seitz[1],
Lauren Law[1,6], Luke Warkentin[1,7], Samantha M. Wilson[1], William I. Atlas[1,8],
Douglas C. Braun[3,5], Matthew R. Sloat[8], M. Tim Tinker[9],
and Jonathan W. Moore[1,3]

[1]Earth to Ocean Research Group, Simon Fraser University
[2]Central Coast Indigenous Resource Alliance, Campbell River, BC
[3]Resource and Environmental Management, Simon Fraser University
[4]Fisheries & Oceans Canada, Cultus Lake Laboratory, Cultus Lake, BC
[5]Ministry of Forests, Lands, Natural Resource Operations, and Rural Development, Smithers, BC
[6]Fisheries & Oceans Canada, Salmonid Enhancement Program, Nanaimo, BC
[7]Fisheries & Oceans Canada, North Coast Stock Assessment, Smithers, BC
[8]Wild Salmon Center, Portland, OR
[9]Ecology and Evolutionary Biology, University of California Santa Cruz

11 May 2022

Contents

*Corresponding author - email: klwilson.ccira@gmail.com

Metapopulation model

Local & metapopulation dynamics

Our metapopulation was defined by a set of P local populations for a species with a one year generation time with time-dynamics that follows birth (i.e., recruitment R), immigration, death, and emigration processes typical to metapopulation theory and tested the role of multiple spatial, temporal, and density-dependent processes (Anderson et al. 2015; Okamoto et al. 2020):

$$N_{i,t} = R_{i,t} + \sum_{\substack{j=1 \\ j \neq i}}^{P} \omega p_{i,j} R_{j,t} - d_{i,t} R_{i,t} - \omega R_{i,t} \tag{S.1}$$

where $N_{i,t}$ was the number of adults in patch i at time t, $R_{i,t}$ was the number of recruits at time t, $\sum_{\substack{j=1 \\ j \neq i}}^{P} \omega p_{i,j} R_{j,t}$ was the number of recruits immigrating into patch i from any other patch, ω was the proportion of local recruits to disperse, $p_{i,j}$ was a distance-dependent dispersal function, and $d_{i,t}$ was the proportion of recruits that die due to disturbance regime.

Local patch recruitment at time t depended on adult densities at *t-1* and followed a reparameterized Beverton-Holt function (Walters & Martell 2004; Forrest et al. 2010):

$$R_{i,t} = \frac{\alpha_i N_{i,t-1}}{1 + \dfrac{\alpha_i - 1}{\beta_i} N_{i,t-1}} \epsilon_{i,t} \tag{S.2}$$

where α_i was the recruitment compensation ratio, β_i was local patch carrying capacity, and $\epsilon_{i,t}$ was lognormally distributed deviates to introduce stochastic recruitment dynamics.

Resource monitoring often occurs at the scale of the whole metapopulation by aggregating abundances among local populations to (Anderson et al. 2015; Moore et al. 2021), hence we define metapopulation adults as:

$$A_t = \sum_{i=1}^{P} N_{i,t} \tag{S.3}$$

with metapopulation recruits:

$$K_t = \sum_{i=1}^{P} R_{i,t} \tag{S.4}$$

Monitoring at the scale of the whole metapopulation can produce productivity relationships that aggregates the population dynamics and productivity among all local populations. For example, take a two patch metapopulation model that varies α_i and β_i parameters where:

```
alpha <- c(2, 4)
beta <- c(100, 200)
```

Here, recruitment compensation from local patches α_i gets averaged across the metapopulation leading to an average compensation ratio $\bar{\alpha}$ of 3. Likewise, the total carrying capacity of the metapopulation $\bar{\beta}$ becomes the summation of local patch carrying capacities $\sum \beta_i$, which was 300. This scale of monitoring generates the following local patch and metapopulation dynamics:
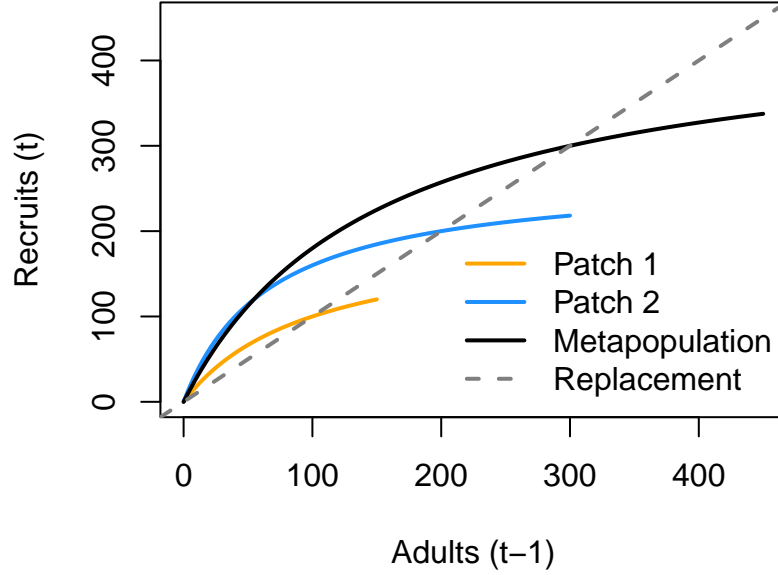
Figure S1: Metapopulation and local patch recruitment dynamics.

Creating the spatial networks

The next aspect to our metapopulation model was connecting the set of patches to one another (Yeakel et al. 2014). We need to specify the number of patches, their arrangements (i.e., connections), and how far apart they are from one another. We followed some classic metapopulation and source-sink arrangements to create four networks that generalize across a few real-world topologies: a linear habitat network (e.g., coastline), a dendritic or branching network (e.g., coastal rivers), a star network (e.g., mountain & valley, or lake with inlet tributaries), and a grid network (e.g., grasslands).

To make networks comparable, each spatial network type needs the same leading parameters (e.g., number of patches P and mean distance between neighboring patches $\bar{d}$). In this case, we set P to `16` and $\bar{d}$ to `1` unit (distance units are arbitrary). We used the `igraph` package (Csardi & Nepusz 2006) and some custom code to arrange our spatial networks as the following:
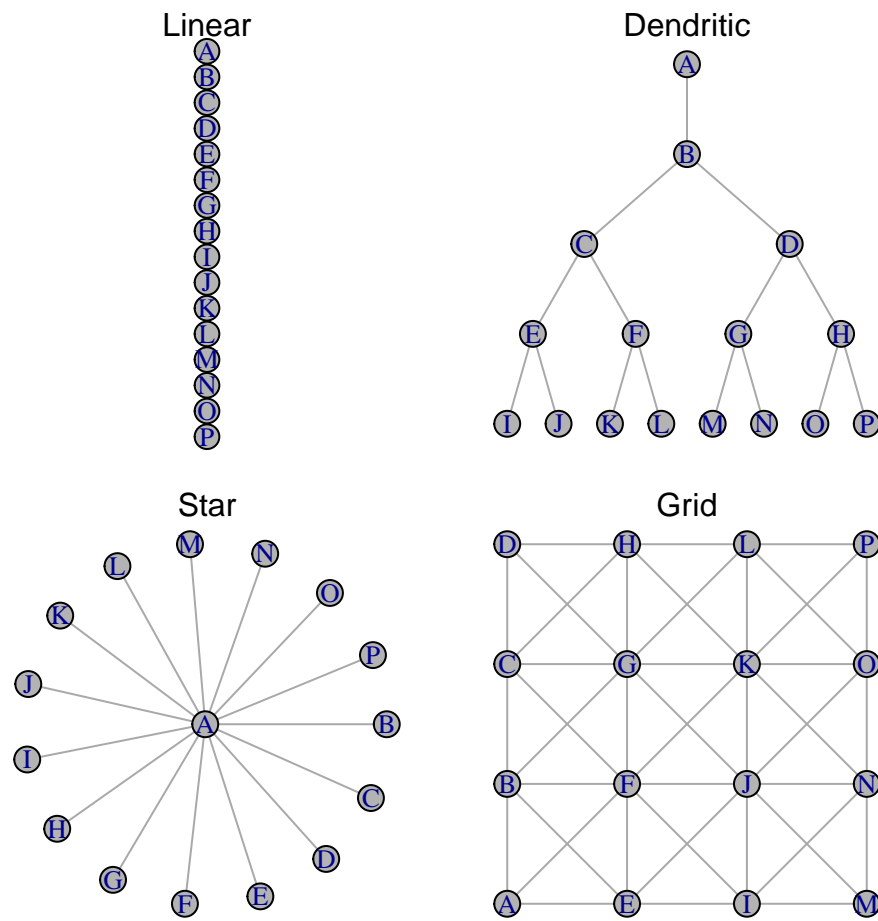
Figure S2: Four spatial network topologies.

57   Note that distances between neighbor patches in the above networks are equal.

An example dispersal matrix for the grid network:

```
##    A B E F C G D H I J K L M N O P
## A 0 1 1 1 2 2 3 3 2 2 2 3 3 3 3 3
## B 1 0 1 1 1 1 2 2 2 2 2 2 3 3 3 3
## E 1 1 0 1 2 2 3 3 1 1 2 3 2 2 2 3
## F 1 1 1 0 1 1 2 2 1 1 1 2 2 2 2 2
## C 2 1 2 1 0 1 1 1 2 2 2 2 3 3 3 3
## G 2 1 2 1 1 0 1 1 2 1 1 1 2 2 2 2
## D 3 2 3 2 1 1 0 1 3 2 2 2 3 3 3 3
## H 3 2 3 2 1 1 1 0 3 2 1 1 3 2 2 2
## I 2 2 1 1 2 2 3 3 0 1 2 3 1 1 2 3
## J 2 2 1 1 2 1 2 2 1 0 1 2 1 1 1 2
## K 2 2 2 1 2 1 2 1 2 1 0 1 2 1 1 1
## L 3 2 3 2 2 1 2 1 3 2 1 0 3 2 1 1
## M 3 3 2 2 3 2 3 3 1 1 2 3 0 1 2 3
## N 3 3 2 2 3 2 3 2 1 1 1 2 1 0 1 2
## O 3 3 2 2 3 2 3 2 2 1 1 1 2 1 0 1
## P 3 3 3 2 3 2 3 2 3 2 1 1 3 2 1 0
```

Dispersal

Dispersal from patch i into patch j depends on constant dispersal rate ω (defined as the proportion of total local recruits that will disperse) and an exponential distance-decay function between i and j with distance cost to dispersal m following Anderson et al. (2015):

$$E_{i,j,t} = \omega R_{i,t} p_{i,j} \tag{S.5}$$

where $E_{i,j}$ was the total dispersing animals from patch i into patch j resulting from dispersal rate ω, total number of local recruits $R_{i,t}$, and probability of dispersal between patches $p_{i,j}$:

$$p_{i,j} = \frac{e^{-md_{i,j}}}{\displaystyle\sum_{\substack{j=1 \\ j \neq i}}^{P} e^{-md_{i,j}}} \tag{S.6}$$

where $d_{i,j}$ was the pairwise distance between patches, m was the distance cost to dispersal. The summation term in the denominator normalizes the probability of moving to any patch to between 0 and 1 with the constraint that dispersers cannot move back into their home patch (i.e., $j \neq i$. With $\bar{d} = 1$, $m = 0.5$, $\omega = 0.1$, $R_{i,t} = 100$ in a linear network):
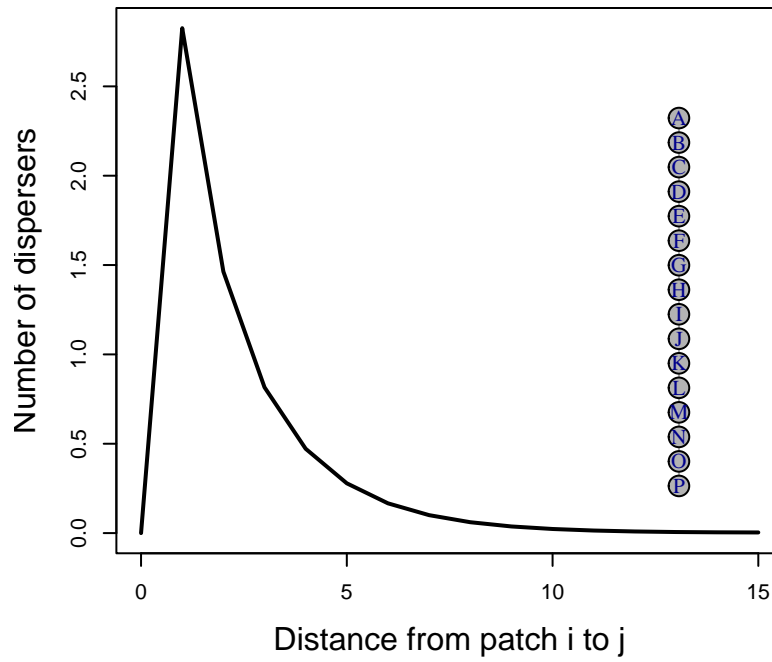
Figure S3: Example dispersal patterns across linear network.

Disturbance regimes

In all scenarios, disturbance was applied after 50 years of equilibrating the metapopulation at pristine conditions. We then applied the disturbance regime at year 50 (the regime varied from *uniform*, *localized, even*, and *localized, uneven* - see *Scenarios* below). Disturbance immediately removed a fixed proportion of the metapopulation adults at that time (i.e., 0.9 of $A_{t=50}$). Once applied, the metapopulation was no longer disturbed and spatio-temporal recovery dynamics emerged from these conditions given the ecological scenarios of network complexity, dispersal rate, spatio-temporal correlations, local patch demographies, and magnitude of stochastic variance.
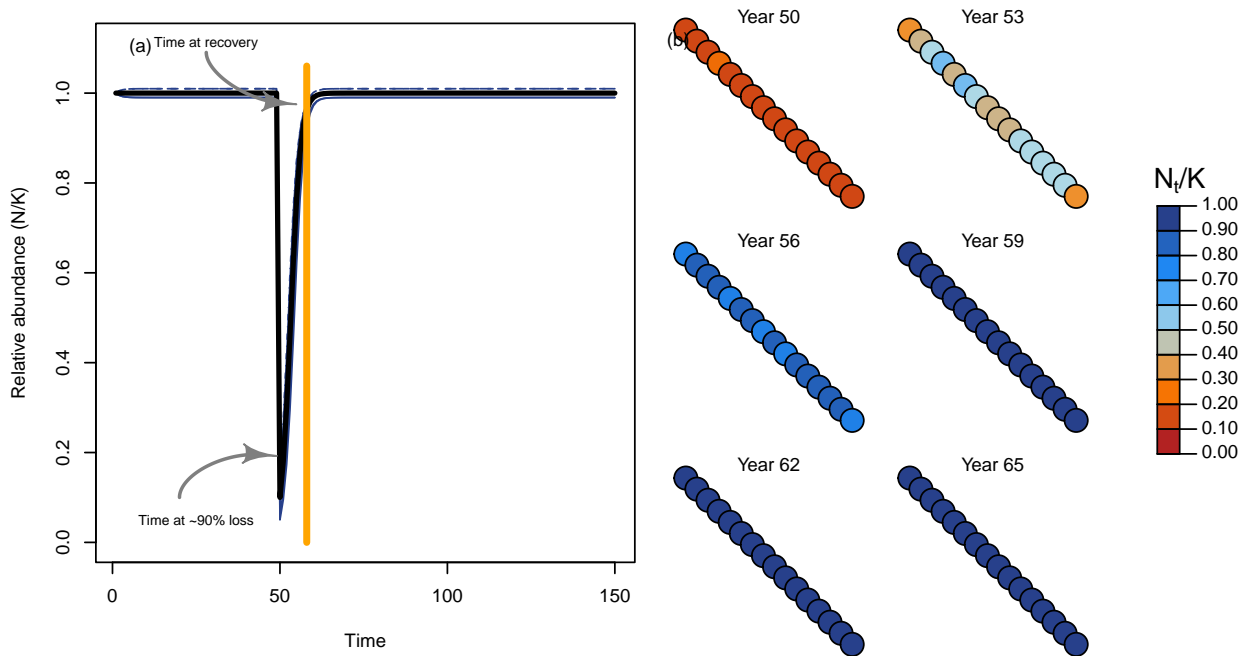

Figure S4: Recovery regime of metapopulation with linear topology through time (a) and space (b).

Recruitment stochasticity

Our model allowed for stochastic recruitment that followed a lognormal distribution with average variation in recruitment of σ_R. In cases with stochastic recruitment, the deterministic recruitment in eq. S.4 becomes:

$$R_{i,t} = \frac{\alpha_i N_{i,t-1}}{1 + \dfrac{\alpha_i - 1}{\beta_i} N_{i,t-1}} e^{\left(\epsilon_{i,t} - \frac{\sigma_R^2}{2}\right)} \tag{S.7}$$

where lognormal deviates for each patch i at time t were drawn from a multivariate normal distribution (MVN) with bias correction $\dfrac{\sigma_R^2}{2}$. If σ_R was low, then metapopulation dynamics approach the deterministic case. In some scenarios, we evaluated the role of spatially and/or temporally correlated deviates among local patches to model potential common drivers affecting metapopulation dynamics (e.g., Moran effects). Expected recruitment deviates followed a first-order autoregression model such that:

$$\epsilon_{i,t} = \rho_T \epsilon_{t-1} + MVN(\mu = 0, \Sigma = \sigma_R^2(1 - \rho_T^2)e^{(-\rho_S D_{i,j})}) \tag{S.8}$$

where ρ_T was temporal correlation (bounded $0 - 1$) ρ_S was rate of distance-decay in spatial correlation (bounded $0 - \infty$ with higher values leading to independent patches). If ρ_T was 0 and ρ_S was high, then annual recruitment deviates were independent. We modelled the initial conditions for autoregressive recruitment deviates $\epsilon_{i,1}$ by drawing from a stationary normal distribution with mean $\mu = 0$ and variance σ_R^2 such that:

$$\epsilon_{i,1} \sim N(\mu = 0, \sigma = \sigma_R) \tag{S.9}$$

We illustrate the effects of four kinds of recruitment deviates below using the same random number generator seed:
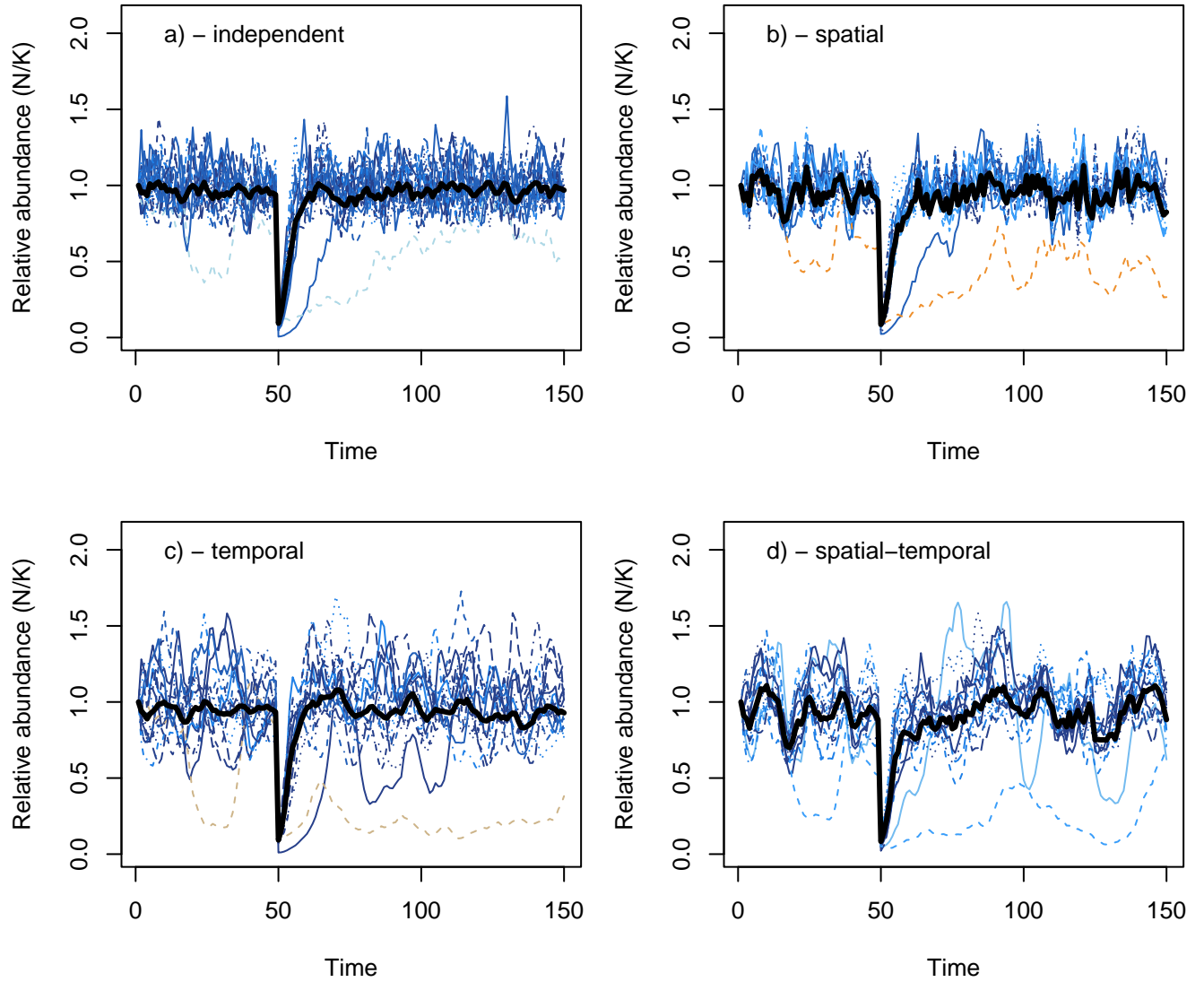
Figure S5: Metapopulation dynamics with independent (a), spatially correlated (b), temporally correlated (c), and spatio-temporally correlated (d) recruitment deviates. Black line indicates metapopulation, and dashed lines indicate local patches with red and blue relating to abundances after 100 years post-disturbance were less than or greater than 1.0 pre-disturbance, respectively.

Post-disturbance outcomes

We measured the following post-disturbance outcomes to track the temporal and spatial recovery regime of the metapopulation.

1. Non-recovery (a) & recovery rate (b) after disturbance:

    a. Non-recovery rate was defined as the % of simulations where metapopulation abundance failed to recover to `1.0` of the average pre-disturbance abundance for `5` consecutive years post-disturbance. This "non-recovery rate" reflects the risk of a long-term state shift in metapopulation dynamics after disturbance in the face of stochasticity.
    b. Recovery rate represents the proportional post-disturbance recovery towards metapopulation carrying capacity gained per year (1 year = 1 generation in our models). Recovery rate was calculated as $1 - T_{recovery}/T_{sim}$ where the recovery time, $T_{recovery}$, was the number of years/generations it took for the metapopulation to reach five consecutive years pre-disturbance abundance. Recovery rate captures how quickly the aggregate metapopulation recovers from disturbance but doesn't take into account whether any given local patches recover to their pre-disturbance capacity nor did it allow for any

116   uncertainty around recovery criteria.

117 2. Patch occupancy - the mean number of patches with `>0.1` local carrying capacity after disturbance in the
118   short-term (5 years), medium-term (10 years), and long-term (25 years). This value characterizes the
119   expected risk of spatial contractions or local patch collapses, and reflects how interactions between spatial
120   structure, disturbance, and dispersal shape source-sink dynamics and the ability to provide (or not) rescue
121   effects and recover local patches.

122 3. The ratio of expected maximum surplus production (we term *MSY*) to true maximum surplus production
123   summed across all patches from fitted stock-recruitment model to aggregate across metapopulation such that:

$$\Delta_{MSY} = \frac{M\hat{S}Y_M}{\sum_{i=1}^{P} MSY_i} \tag{S.10}$$

124   A value of 1.0 would indicate that the disturbed metapopulation can sustain itself against the same
125   disturbance regime as the sum of each patch independently. In other words, was the metapopulation more
126   than ($\Delta_{MSY} > 1.0$), less than ($\Delta_{MSY} < 1.0$), or equal to the sum of its parts ($\Delta_{MSY} = 1.0$). We detail how *MSY*
127   was estimated further below.

Monitoring & management at aggregate-scale

129 While true metapopulation dynamics emerge from local patch dynamics and dispersal in S.1, natural resource
130 managers often monitor and manage at the scale of the metapopulation. Hence, management at this scale
131 inherently defines the stock-recruitment dynamics of the aggregate complex of patches (i.e., metapopulation) as:

$$K_t = \frac{\hat{\alpha}_t A_{t-1}}{1 + \frac{\hat{\alpha}_t - 1}{\hat{\beta}_t} A_{i,t-1}} \tag{S.11}$$

132 where $\hat{\alpha}_t$ was the estimated compensation ratio averaged across the metapopulation at time t and $\hat{\beta}_t$ was the
133 estimated carrying capacity of the entire metapopulation. Necessarily, these estimates emerge from monitoring
134 data collected across all patches and are sensitive to the quality of the data and how local patches perform through
135 time. For example, temporal shifts in productivity regimes may be masked if most of the data were sampled before
136 the regime shift. To help surmount these issues, modern resource assessments use data weighting and penalties (i.e.,
137 priors) when fitting models to data.

138 In our assessment, we weighted recent years of sampling over more distant years such that:
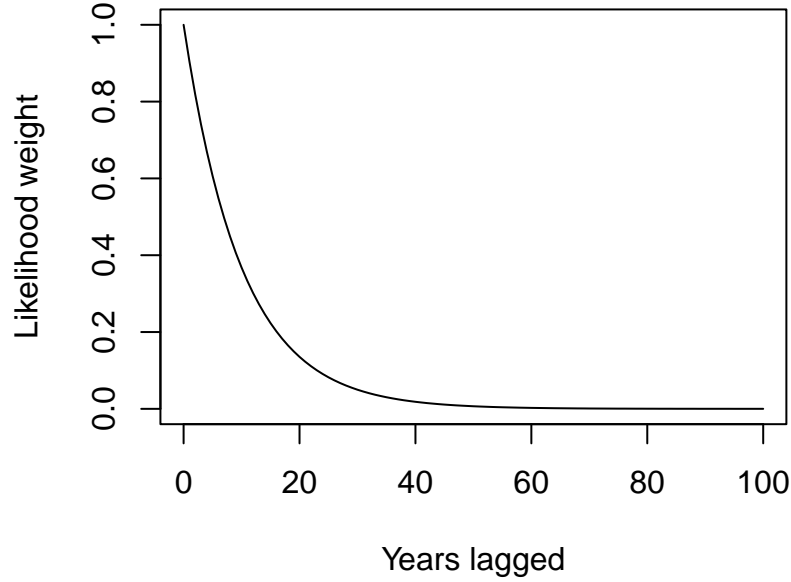
Figure S6: Likelihood weighting for samples collected over time from current year of sampling.

139 This forward-weighting approach increased the sensitivity of the monitoring sub-model to detect demographic
140 changes in the post-disturbance recovery regime. Data-weighting is increasingly being used in resource monitoring,
141 although how weights are developed and applied to data is a case-by-case basis.

142 Furthermore, we used penalized normal likelihoods on both $\hat{\alpha}_t$ and $\hat{\beta}_t$ such that:

$$\hat{\alpha}_t \sim N(\mu = \hat{\alpha_{t-1}}, \sigma = 3\hat{\alpha_{t-1}}) \tag{S.12}$$

143 and

$$\hat{\beta}_t \sim N(\mu = \hat{\beta_{t-1}}, \sigma = 3\hat{\beta_{t-1}}) \tag{S.13}$$

144 where $\mu = \hat{\alpha_{t-1}}$ and $\mu = \hat{\beta_{t-1}}$ represents the best estimates from the previous assessment and the 3 in the σ term
145 represents a 300% coefficient of variation. We used these penalized likelihoods to fit the above aggregate
146 stock-recruitment model with *lognormal* error to the metapopulation stock-recruit data collected at time *t*. We
147 used the following function and fitted to the below θ parameters (termed `theta` in the function `optim()` using the
148 L-BFGS-B optimizer with a lower bound on $\hat{\alpha}$ of `1.01` (i.e., constrained to be at least above replacement).

```
SRfn <- function(theta, data, lastYr) {
    a.hat <- theta[1]
    b.hat <- exp(theta[2])
    sd.hat <- exp(theta[3])
    rec.mean <- (a.hat * data$spawners)/(1 + ((a.hat - 1)/b.hat) * data$spawners)
    # negative log likelihood on recruitment parameters
    nll <- -1 * sum(dlnorm(data$recruits, meanlog = log(rec.mean), sdlog = sd.hat,
        log = TRUE) * data$weights, na.rm = TRUE)
    # penalized likelihood on estimated alpha
    penalty1 <- -dnorm(a.hat, lastYr$alphaLstYr, 4 * lastYr$alphaLstYr, log = TRUE)
    # penalized likelihood on estimated carrying capacity
```

```
        penalty2 <- -dnorm(b.hat, lastYr$metaKLstYr, 4 * lastYr$metaKLstYr, log = TRUE)
        jnll <- sum(c(nll, penalty1, penalty2), na.rm = TRUE)
        return(jnll)
}
```

149 This above function allows us to assess the bias in $\hat{\alpha}_t$, $\hat{\beta}_t$, and $\hat{K}_t$ compared to true $\bar{\alpha}$, $\bar{\beta}$, and K_t across the
150 metapopulation. This then allows us to see how much information management & monitoring programs were
151 missing when they assess metapopulations at the aggregate (rather than local) scales.

Finding maximum sustainable yield

153 Resource managers measure productivity with a variety of performance reference points (Forrest et al. 2010). One
154 of the most widely used metrics, commonly called *Maximum Sustainable Yield* in fisheries and other harvest
155 literature (MSY), relates to the largest loss the population can sustain over an indefinite period of time that
156 maximizes its ability to replenish itself. Under density-dependent growth, individuals' growth, survival, and
157 reproduction at low population densities are not constrained by limited resources, but overall production is low
158 because there are few individuals. At high densities, limited resources increasingly constrain individual's
159 reproductive success until the population reaches carrying capacity, and overall production drops to zero because
160 per-capita success is low. However, at some intermediate densities, both per-capita and overall production is high,
161 and population growth is at its maximum point due to the large number of reproducing individuals. At this point,
162 there is the maximum surplus of individuals produced above replacement that can help to withstand disturbance or
163 harvest regimes and contribute to future recovery, either through increasing local patch densities or by emigrating
164 neighboring patches providing "rescue effects".

165 Under Beverton-Holt or Ricker density-dependent recuitment, however, there exists no analytical solution for
166 calculating MSY. Therefore, we used numerical methods and a one dimensional root finder to iteratively search for
167 the population mortality that maximized surplus production in the metapopulation. We term this mortality F_{MSY}
168 and can use this mortality value to calculate maximum surplus production MSY, the adult densities that produce
169 MSY (termed N_{MSY}), and the recruits that result from this (termed R_{MSY}).

```
# uniroot numerical search
yieldRoot <- function(alpha, beta, Fcur, model) {
    Ucur <- 1 - exp(-Fcur)
    if (model == "Beverton-Holt") {
        # population model is R ~ (CR * S)/(1+(CR-1)/K * S): reparameterized
        # Beverton-Holt
        adults <- beta * exp(-Fcur)
        recruits <- (alpha * adults)/(1 + ((alpha - 1)/beta) * adults)
        yield <- recruits - adults
    }
    if (model == "Ricker") {
        # population model is R ~ CR * S * e(-log(CR)/K * S): reparameterized
        # Ricker
        adults <- beta * exp(-Fcur)
        recruits <- alpha * adults * exp((-log(alpha)/beta) * adults)
        yield <- recruits - adults
    }
    return(list(recruits = recruits, adults = adults, yield = yield))
}

# Return approximate gradient for integral
fun_yield <- function(Fcur, alpha, beta, delta, model) {
    y1 <- yieldRoot(alpha = alpha, beta = beta, Fcur = Fcur - delta/2, model = model)$yield
    y2 <- yieldRoot(alpha = alpha, beta = beta, Fcur = Fcur + delta/2, model = model)$yield
    approx.gradient <- (y2 - y1)/delta
    return(approx.gradient)
}

# uniroot search for optimal yield and Fmsy
findMSY <- function(alpha, beta, Npatches, model) {
    F_msy <- NULL
    for (i in 1:Npatches) {
        a_p <- alpha[i]
        b_p <- beta[i]
        F_msy[i] <- uniroot(fun_yield, interval = c(0, 1), extendInt = "yes", alpha = a_p,
            beta = b_p, delta = 1e-04, model = model)$root
    }
    MSY <- sapply(1:Npatches, function(x) {
        yieldRoot(alpha = alpha[x], beta = beta[x], Fcur = F_msy[[x]][1], model = model)
```

```
    })
    return(list(F_msy = F_msy, MSY = MSY))
}
```

Scenarios

We tested all combinations of the following eight processes (below) and ran `100` iterations per scenario to estimate the mean for each of the above outcomes.

1. Homogenous and spatially variable recruitment compensation ratio across patches, i.e. intrinsic rate of population growth (α_i).

2. Homogenous and spatially variable local carrying capacity across patches, i.e. asymptote of expected recruits at high adult densities (β_i)

3. Disturbances where a proportion of individuals removed from metapopulation (e.g., `0.90`) occurs.

   a. *uniform* - random individuals removed at equal vulnerability across all patches.
   b. *localized, even* - random individuals removed from randomly selected subset of patches (as long as the target individuals lost in the metapopulation can be achieved in that subset of patches)
   c. *localized, uneven* - total extirpation of randomly selected subset of patches (as long as the target individuals lost in the metapopulation can be achieved in that subset of patches)

4. Density-independent dispersal rates ω from 0 to 5% of individuals within a patch will disperse.

5. Topology of the spatial networks with linear, dendritic, star, and grid networks. Each network with $P = 16$ and distance between patches $\bar{d} = 1$.

6. Stochastic recruitment deviates from low, medium, high coefficient of variation on lognormal error. Generate stochasticity in time-dynamics via random recruitement deviates away from expected.

7. Temporal correlation in recruitment deviates from low, medium, high correlation (i.e., good year at time t begets good year at time *t+1*).

8. Spatial correlation in recruitment deviates among patches from low, medium, to high correlation (i.e., neighboring patches go up or down together).

Example results

We demonstrate our metapopulation model with an example outcome for a linear network composed of `16` patches, a dispersal rate of `0.01` and a high enough dispersal cost such that individuals are only willing to move to their closest neighboring patches. This limits the strength of potential rescue effects. For this example, patches varied in their productivity and carrying capacity but will have deterministic population dynamics.
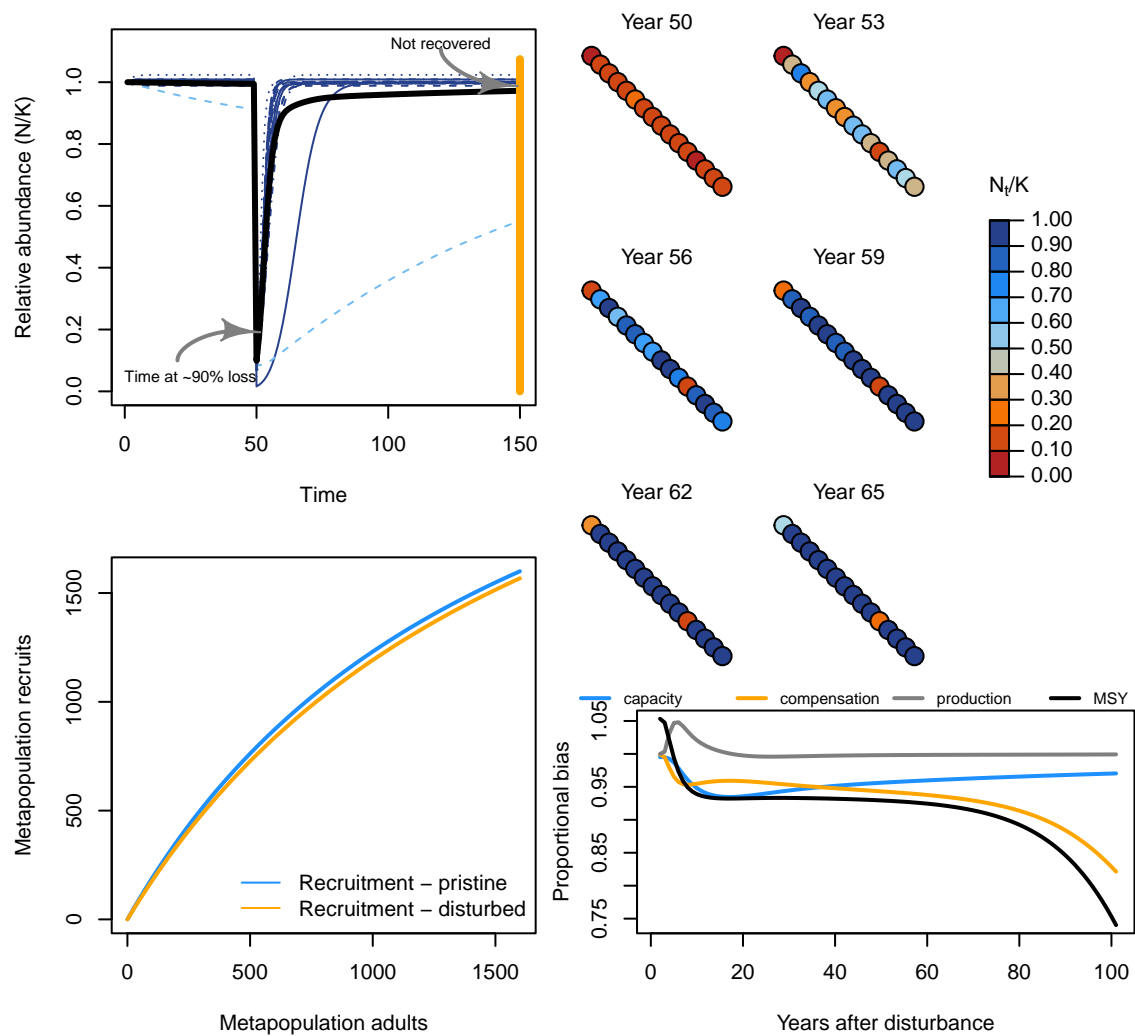
Figure S7: Example iteration of spatial recovery regime of metapopulation with linear topology through time (top left) and space (top right). Recruitment dynamics before and 10 years after disturbance (bottom left). Relative bias in aggregate-scale estimates of carrying capacity, compensation ratio, and recruitment production in recovery phase (bottom right).

197   We can then contrast this with a different network shape, like a dendritic network.
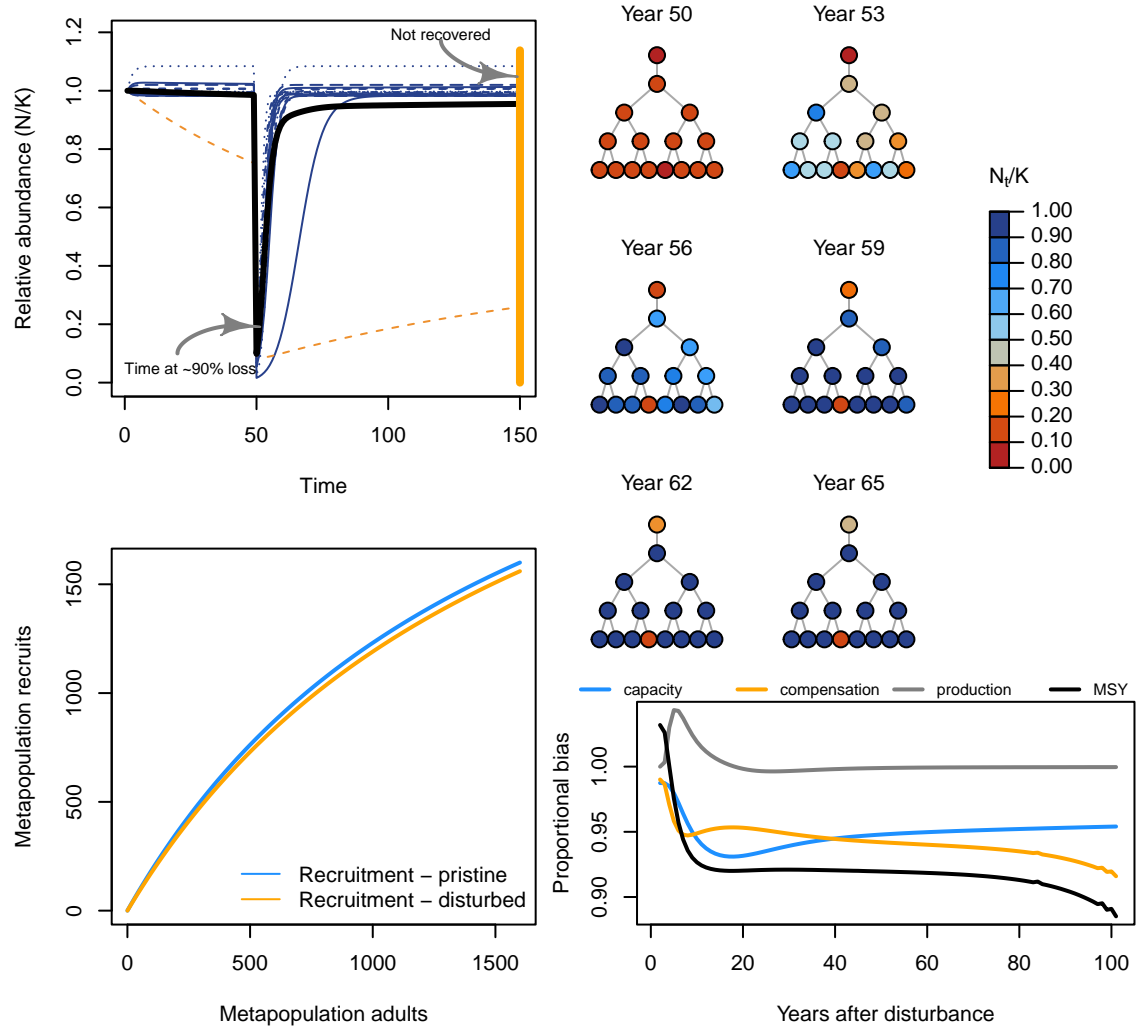

Figure S8: Example iteration of spatial recovery regime of metapopulation with dendritic topology.

198   Now, let's add some stochasticity to recruitment and see how this affects the recovery regime.
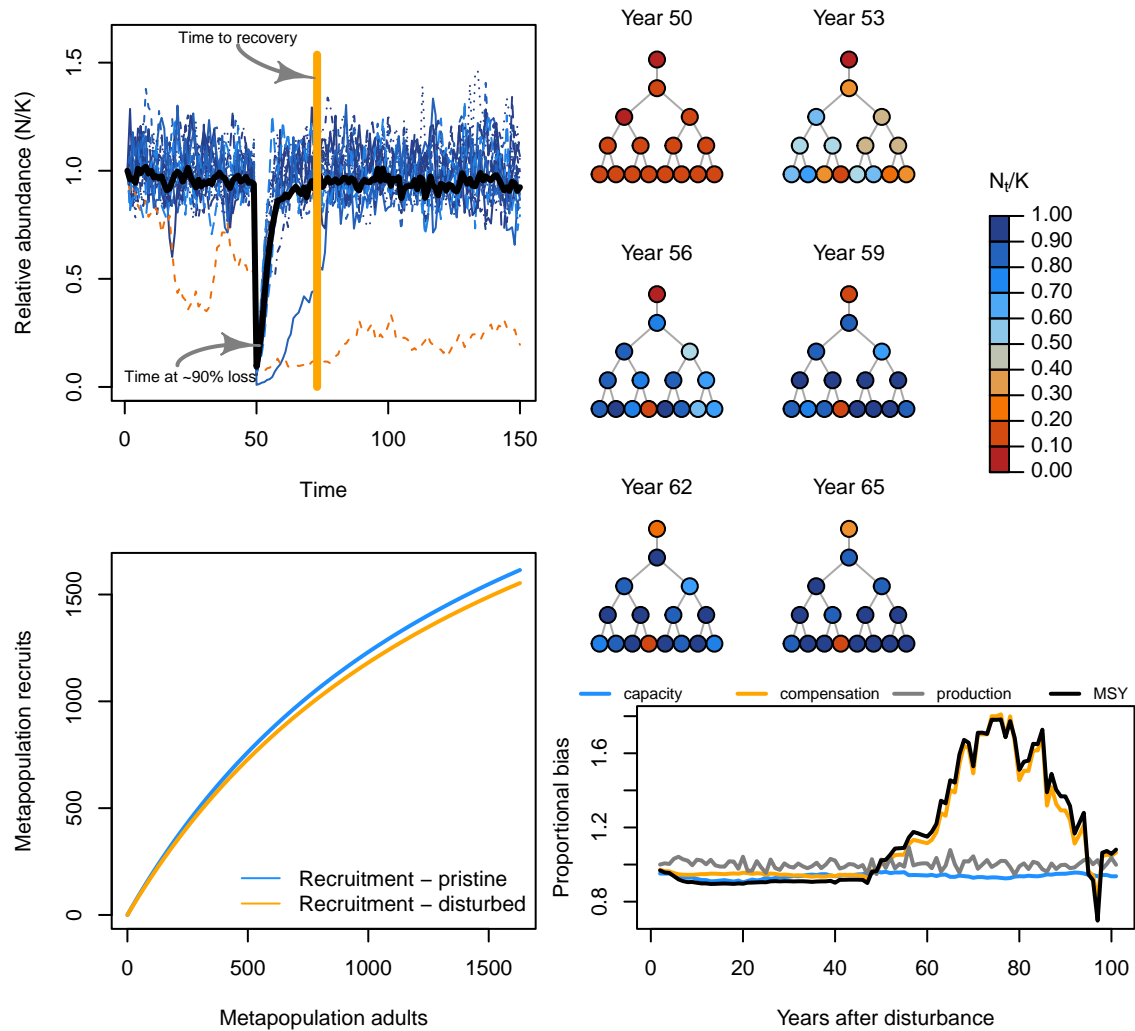

Figure S9: Example iteration of spatial recovery regime of stochastic metapopulation.

¹⁹⁹ Next, we can contrast with a disturbance regime where the disturbance is concentrated on local patches that can
²⁰⁰ be completely extirpated (rather than the disturbance being applied proportionally across all patches e.g., a
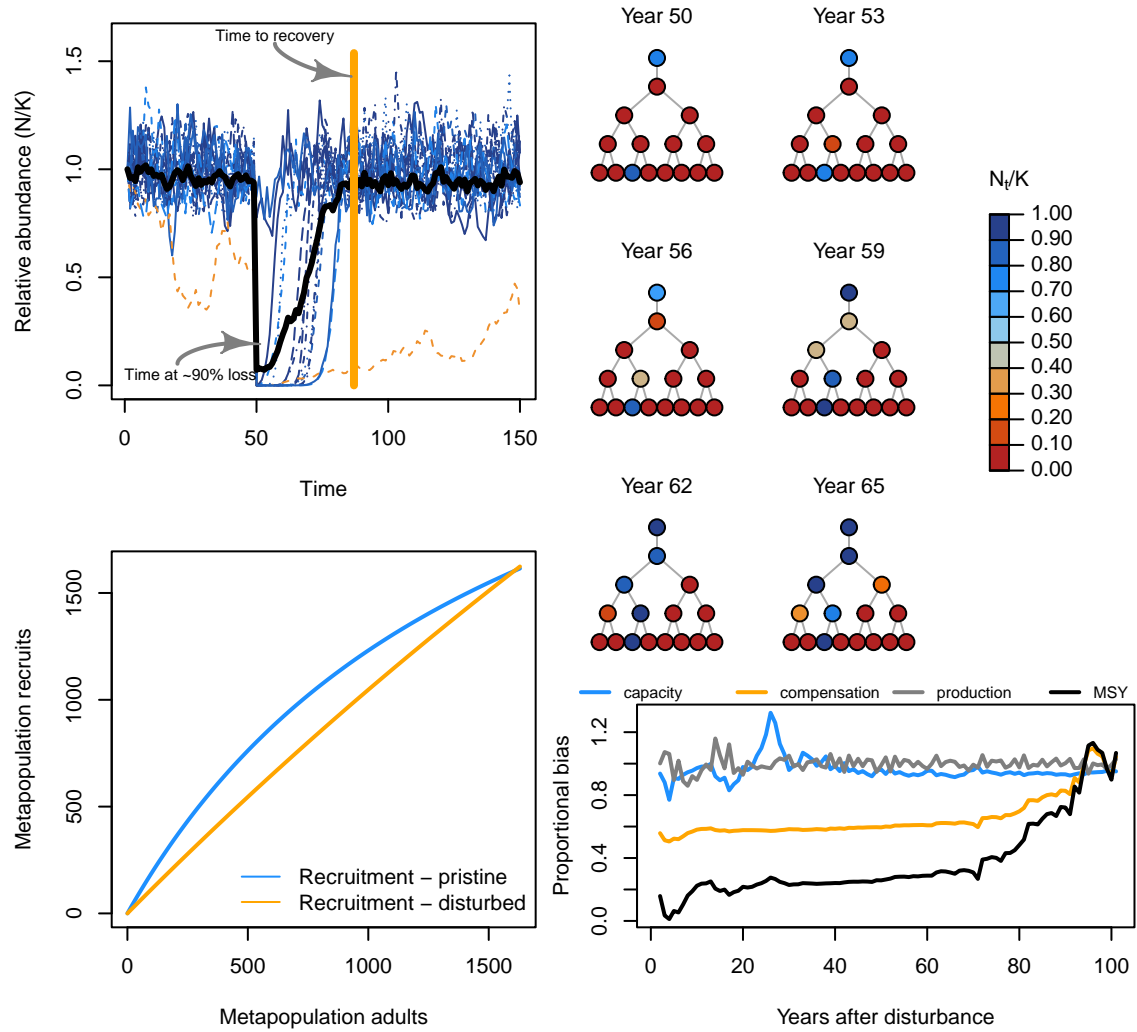²⁰¹ mixed-stock fishery).

Figure S10: Example iteration of spatial recovery regime of stochastic metapopulation.

General patterns

Effects of disturbance regime

The strongest lever influencing recovery in our simulated metapopulations was, by far, the characteristics of the disturbance regime. Specifically, the degree to how locally concentrated the disturbance was on the set of patches was more influential than variable density dependence, dispersal rates, or network topology. This was surprising and not expected in our initial hypotheses. Localized disturbances increased the risk of spatial contraction, reduced recovery rates and aggregate compensation, and increased the risk of a long-term state shift. By altering aggregate compensation, localized disturbance reduced the surplus production of the metapopulation. In other words, through changes in source-sink dynamics, metapopulations under localized disturbance acted less than the sum of their parts – the more localized the impacts, the worse these effects. Uniform disturbances generally left the metapopulation dynamics unaffected with few ecological surprises. These above spatial and temporal recovery processes also appeared tied to one another such that changes to any of them had feedbacks with other recovery metrics.
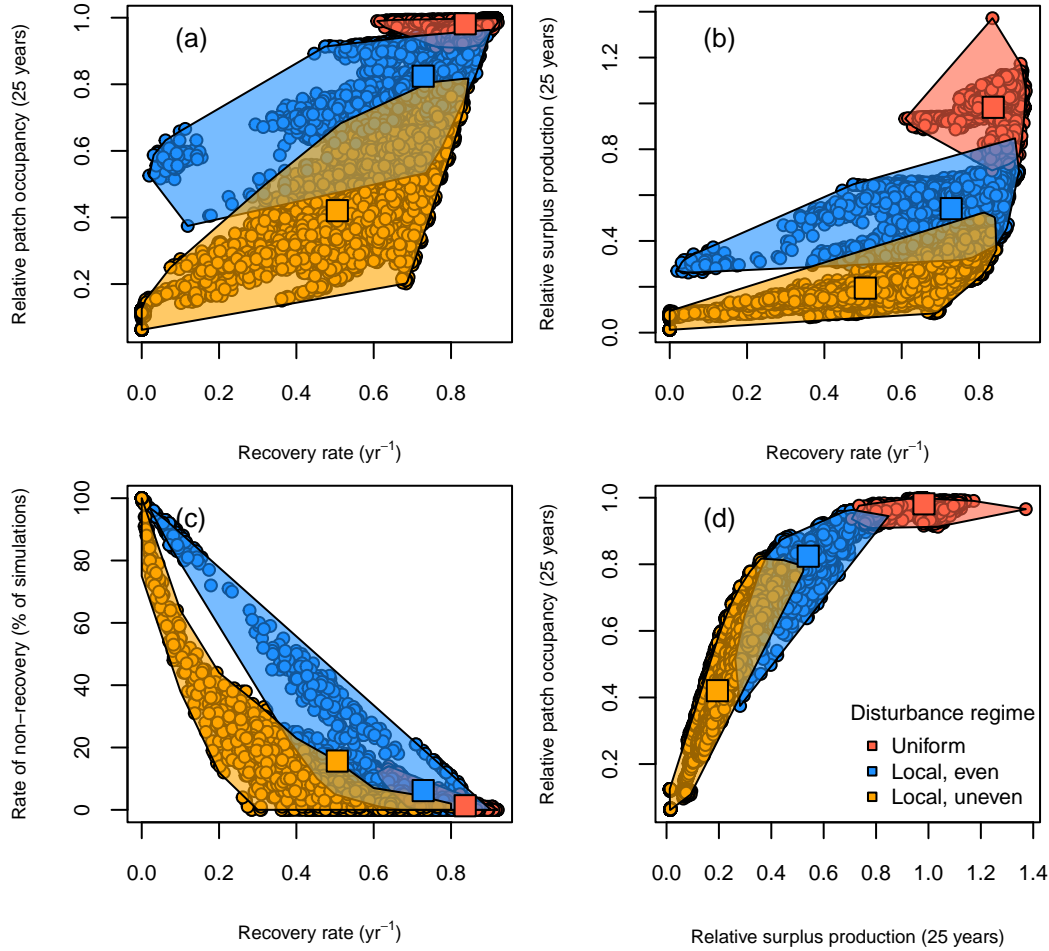

Figure S11: Spatial and temporal recovery patterns along disturbance regimes across all scenarios.

Role of network structure & despersal

We now show some general patterns in how variable patch demographic rates, network structure, dispersal, disturbance, recruitment stochasticity, and spatio-temporal correlations variation affects metapopulation *recovery rates*, *maximum sustainable yield* (analagous to the maximum rate of loss the system can sustain), and *collapse rate* (i.e, the number of simulations where the metapopulation fails to recover), and *patch occupancy* (i.e., number of patches with local abundance <10% of pre-disturbance).
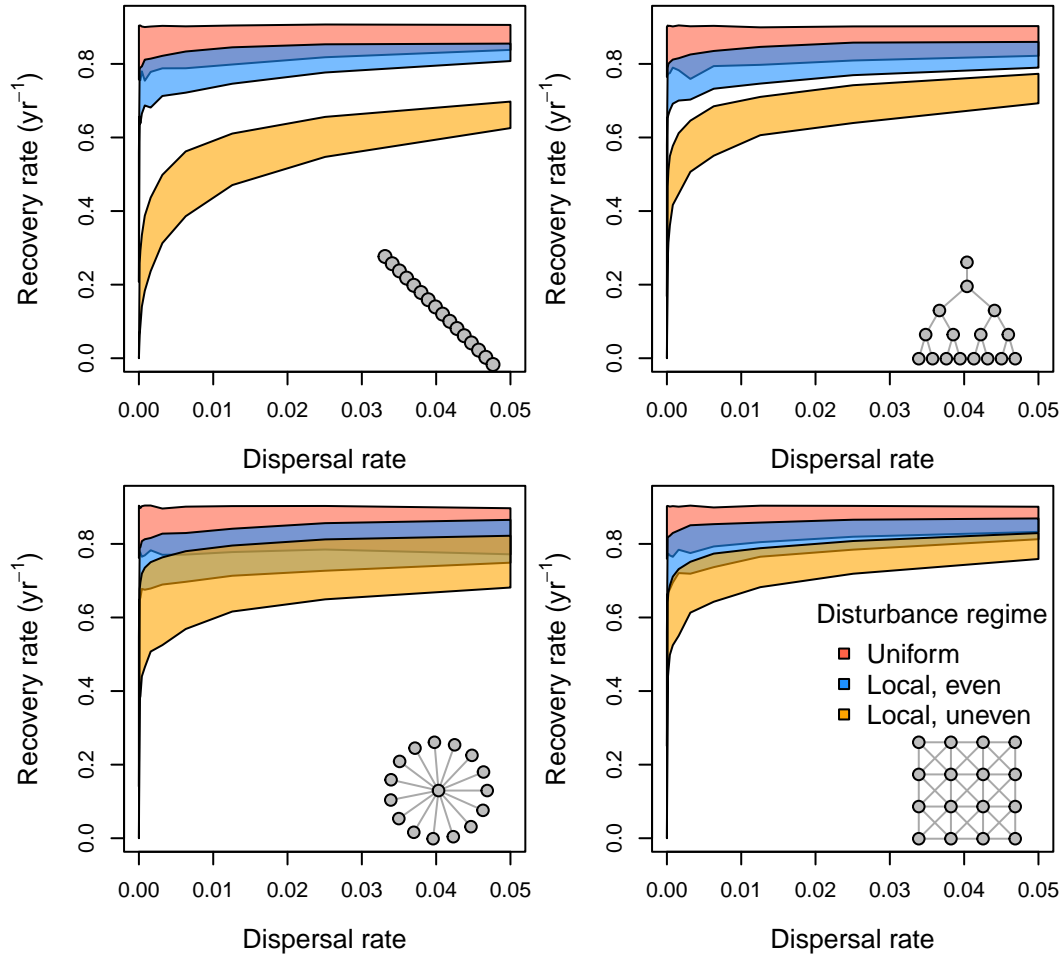

Figure S12: Metapopulation recovery rates along gradients of network configuration, dispersal rates, and spatial distribution of disturbance. The shaded region describes the interquartile range across all scenarios.

Dispersal, landscape structure, and local density-dependence also affected metapopulation recovery patterns in three key ways, though to a lesser extent. First, recovery rates increased with increased dispersal. However, this effect was nonlinear with diminishing benefits of dispersal occurring at ~1-3%, depending on spatial structure and disturbance. Second, more linearized networks had slower recovery times than more connected networks suggesting that rescue effects take some time to cascade through the entire network of patches; but this interacted with the disturbance regime as only local, extirpation exhibited this change in any substantial manner. Last, diversity in local patch compensation and carrying capacities tended to slow metapopulation recoveries - this effect interacted with other factors like stochasticity.

Figure S13: Effects of variable local patch productivities on metapopulation recovery across all scenarios.

Surprising ecological outcomes

Metapopulation recovery regimes emerged from a complex interplay of density-dependent productivity (shown in Figure 6 of the main text), network structure (shown here), dispersal, and disturbance regimes. Overall, clustering analyses of our model results found evidence for six common outcomes: (1) resilient recovery – metapopulation recovery <10 years, (2) slow recovery – metapopulation recovery >10 years and no other surprise, (3) lost capacity – long-term maximum surplus production <50% before disturbance, (4) hidden collapses – metapopulation recovered (or was recovering) but 50% of patches remain unoccupied, (5) spatial contraction – >25% of patches remain unoccupied and (6) critical risk – metapopulation abundance remains <10% of pre-disturbance. Resilient recovery regimes were most common when disturbance was evenly applied across the network and local patches were identical. Any localized disturbances could create ecological surprises, and the frequency of these surprises were often exacerbated when patches were diverse. Localized, even disturbances tended to reduce recovery by 50% compared to even disturbances (from 16 years to 24 years on average). The riskiest recovery outcomes emerged when disturbance was localized and allowed for extirpation. In these scenarios, recovery was slowed by >100% (from 16 years to >32 years on average), surplus production was often reduced by >50%, long-term patch occupancy was reduced by >35%. Last, note that linear networks tended to have higher risks for long-term spatial contractions.
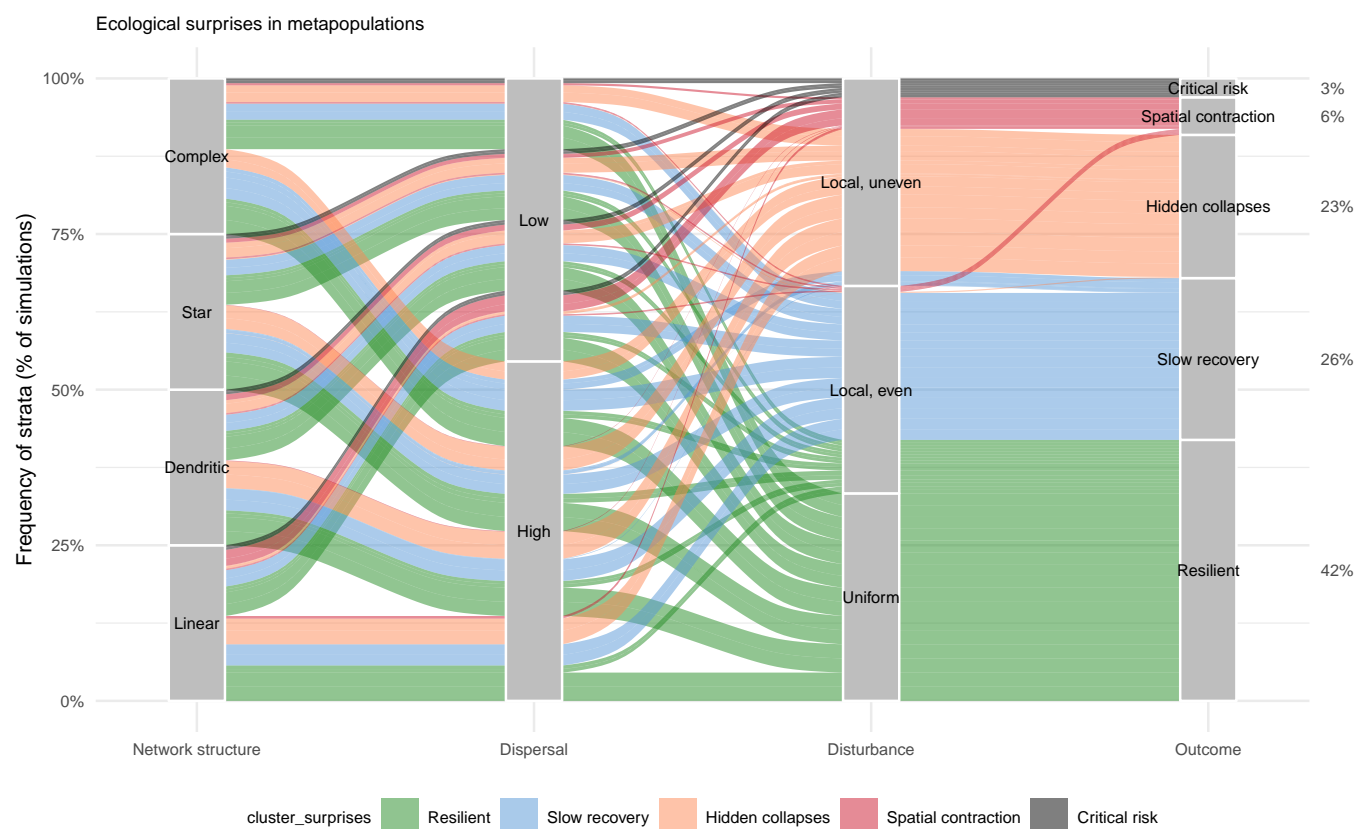

Figure S14: Interplay between network structure, disturbance, and dispersal can lead to suprising recovery outcomes.

References

Anderson, S.C., Moore, J.W., McClure, M.M., Dulvy, N.K. & Cooper, A.B. (2015). Portfolio conservation of metapopulations under climate change. *Ecological Applications*, 25, 559–572.

Csardi, G. & Nepusz, T. (2006). The igraph software package for complex network research. *InterJournal*, Complex Sy, 1695.

Forrest, R.E., McAllister, M.K., Dorn, M.W., Martell, S.J.D. & Stanley, R.D. (2010). Hierarchical Bayesian estimation of recruitment parameters and reference points for Pacific rockfishes (Sebastes spp.) under alternative assumptions about the stock–recruit function. *Canadian Journal of Fisheries and Aquatic Sciences*, 67, 1611–1634.

Moore, J.W., Connors, B.M. & Hodgson, E.E. (2021). Conservation risks and portfolio effects in mixed-stock fisheries. *Fish and Fisheries*, faf.12567.

Okamoto, D.K., Hessing-Lewis, M., Samhouri, J.F., Shelton, A.O., Stier, A.C., Levin, P.S. & Salomon, A.K. (2020). Spatial variation in exploited metapopulations obscures risk of collapse. *Ecological Applications*, 30, e02051.

Walters, C.J. & Martell, S.J.D. (2004). *Fisheries ecology and management.* Princeton University Press.

257 Yeakel, J.D., Moore, J.W., Guimarães, P.R. & Aguiar, M.A.M. de. (2014). Synchronisation and stability in river
258   metapopulation networks. *Ecology Letters*, 17, 273–283.